Glycerol-silicone adhesives with excellent fluid handling and mechanical properties for advanced wound care applications

Chiaula, V.; Mazurek, P.; Eiler, J.; Nielsen, A. C.; Skov, A. L.

Published in:
International Journal of Adhesion and Adhesives

Link to article, DOI:
10.1016/j.ijadhadh.2020.102667

Publication date:
2020

Document Version
Peer reviewed version

Glycerol-silicone adhesives with excellent fluid handling and mechanical properties for advanced wound care applications

V. Chiaula[a, b], P. Mazurek[a], J. Eiler[b, c], A. C. Nielsen[b], A. L. Skov[a*]

[a] Danish Polymer Centre, Department of Chemical and Biochemical Engineering, Technical University of Denmark, DK-2800 Kgs. Lyngby, Denmark.

[b] GRD Technology – Adhesives, Coloplast A/S, DK-3050 Humlebæk, Denmark.

[c] Department of Chemistry, Technical University of Denmark, DK-2800 Kgs. Lyngby, Denmark.

Keywords: glycerol, silicone, wound care, fluid handling, absorption

[*] Corresponding author: al@kt.dtu.dk

Abstract

Adhesives with improved fluid handling and stable mechanical properties are gaining increasing interest in wound care due to improved wound healing conditions. Silicone adhesives possess in general excellent oxygen permeability but poor liquid water absorption and transport due to their inherent hydrophobicity. Herein, we present a novel glycerol-silicone hybrid adhesive with improved fluid handling properties as a result of the incorporation of relatively monodisperse glycerol droplets distributed homogenously throughout the silicone adhesive. The discrete glycerol droplets promote water absorption when the adhesive comes into contact with an aqueous phase due to the hygroscopic nature of glycerol. Additionally, the adhesives' performance, evaluated in terms of mechanical properties, peel, and tack, is shown not to be compromised by presence of the glycerol droplets, mainly due to the so-called solid stiffening effect introduced by their interfacial energies.

1. Introduction

Increased numbers of patients are affected by wounds and, in particular, chronic wounds [1,2], as a consequence of diabetes and other chronic diseases that may affect wound healing [3]. To avoid chronic wounds and to promote faster healing, it is important to maintain a humid environment in the wound

while at the same time ensure that the surrounding skin is not macerated due to presence of too much liquid (water, sweat, and exudate) in close contact with the wound [4,5]. Currently, many adhesives are far too impermeable to avoid maceration over long periods, and therefore, as an example, holes are implemented into the adhesives to allow for moisture transport via larger microscopic or even macroscopic channels. However, these only help locally and maceration may still occur away from the holes. Also, the implemented holes may collapse over time and deplete. A more dense and homogeneous distribution of highly water conducting channels is therefore required for ideal wound healing.

Pressure sensitive adhesives (PSAs) constitute a widely used class of adhesive material in consumer products [6,7]. For wound care applications, the PSAs must be soft and viscoelastic, yet solid, to adapt to human skin in a comfortable manner [8]. Silicone adhesives are usually off-stoichiometric silicone elastomers that remain close to their gelation threshold (i.e. with a low cross-linking degree) [9,10], and within the field of advanced wound care, silicones are currently the preferred adhesive system due to their gentle skin adhesion properties [11–13]. Their softness and low surface tension facilitate polymer chain mobility on and into the skin, thereby creating a large, intimate contact area on the uneven skin surface [14]. In addition, silicone adhesives do not leave a significant residue on the skin when removed, and therefore they are considered atraumatic [15].

To avoid maceration, a wound care adhesive should allow for effective moisture transmission at the skin-adhesive interface. Due to large mobility of the silicone polymer chains (silicone has a high free volume at room temperature), silicone adhesives have excellent oxygen permeability and a high water vapor transmission rate (WVTR) [8,16], and therefore handle transport of gaseous substances well. However, due to their inherent hydrophobic nature, current silicone adhesive solutions are challenged when it comes to fluid handling, in that basic perspiration from the patient's skin can cause the dressing to lose its adhesive properties and eventually fall off. Failure occurs if the amount of sweat produced by the patient's skin is greater than the sum of absorption capacity and the permeability of the adhesive [17–21].

To overcome the hydrophobicity of the silicone surface, grafting of hydrophilic moieties to the silicone surface has been investigated [22–24]. The resulting increase in water transport is initially large but over time the silicone depletes the hydrophilic surface due to the low surface energy of the hydrophobic silicone by absorbing the hydrophilic groups into the bulk of silicone [25].

Two-phase glycerol-silicone hybrid elastomers which, depending on formulation, possess a bi-continuous or closed cell structure have been thoroughly described by Mazurek *et al* [26]. They can be shaped as thin films, bulk elements and foams [27]. Both constituents furthermore are known to be biocompatible and non-toxic [28–30]. The glycerol-silicone composites are created in a simple manner by providing high shear forces to mixtures of glycerol and silicone prepolymers [26]. In this way, physically stable glycerol-in-silicone emulsions are formed which, upon cross-linking of the silicone phase, form free-standing two-phase elastomers. As reported previously, upon contact with an aqueous phase, the composites absorb significant amounts of water [26,31,32].

The use of glycerol-silicone composites as skin adhesives has not been described before. Herein, we present a novel glycerol-silicone hybrid adhesive with improved fluid handling properties as a result of micrometer-sized glycerol droplets dispersed evenly throughout the silicone adhesive. We find that incorporating glycerol increases the water absorption and permeability of silicone adhesives, thereby making them potential candidates for use as wound care adhesives.

2. Experimental

2.1 Materials

A commercially available two-part system (part A and part B) hydrosilylation-curing MG7-9900 soft silicone adhesive kit was purchased from DowDuPont Inc.™.. Glycerol was kindly provided by Emmelev A/S, Denmark. Perylene (synthesis grade) and sulforhodamine B acid chloride (technical grade) were acquired from Sigma-Aldrich, Denmark. All the components were used as received. Polyethylene terephthalate (PET) and polyurethane (PU) backing films were provided by Mitsubishi Polyester Film (Germany) and by Coveris (UK), respectively. A fluorinated ethylene propylene (FEP) release liner was purchased from Lohmann (UK). A UV-curable negative photoresist polymer film (MX5050) used to create the artificial skin was provided by Dupont (USA).

2.2 Methods

2.2.1 Sample preparation

The two components of the commercial soft silicone adhesive kit were mixed in a 1:1 ratio by weight, as recommended by the manufacturer. Subsequently the desired amount of glycerol was added to the silicone adhesive premix. The abbreviation 'phr', used to describe glycerol content in all compositions, corresponds to glycerol weight per hundred parts of silicone adhesive. So, for example, 10 phr means that 10 g of glycerol was used per 100 g of the silicone adhesive premix. Samples name were formed using the GX pattern, where 'G' and 'X' stand for glycerol and glycerol phr added to silicone adhesive premix, respectively (for instance, G40 is 40 phr of glycerol). The mixtures were stirred for 2 min in two steps: 1 min by hand-mixing with a spatula and 1 min at 3500 rpm with a dual asymmetric centrifuge SpeedMixer DAC 150 FVZ-K (Germany). No additional degassing of the formulations was necessary. The obtained glycerol-in-silicone emulsions were coated at 23 mm/s onto a PET or PU backing film with commercial knives (with gap sizes of 0.4 mm or 0.8 mm) and an RK K Control Coater to obtain adhesives with thicknesses around 0.3 or 0.6 mm. The samples were subsequently cured at 80 ± 1°C for 1 h and then cut in a pre-defined shape. All samples were covered with an FEP release liner after coating, and before any measurement took place, this liner was removed. Adhesive thicknesses were then measured using a digital thickness gauge (Mitutoyo, Germany).

2.2.2 Morphology of glycerol-silicone adhesive and determination of glycerol surface area per volume of adhesive

A Leica DM LB optical microscope was used to investigate the morphologies of the uncured samples, whilst a confocal Leica TCS SP5 X was used to analyse the morphology of cured composites. In order to demonstrate the distribution of glycerol droplets into silicone, we labelled each phase with different colour dyes. Sulforhodamine B and perylene were used to dye the glycerol and the silicone phases, respectively. To determine the glycerol surface area per volume of adhesive, glycerol spherical droplets in the formulation were measured in terms of their diameter by counting the droplets directly from microscopy pictures, using ImageJ software. The detailed calculations are reported in Supplementary Information (SI).

2.2.3 Fluid handling capability of adhesives

To measure the permeability of the adhesives, specimens of area (A) 10 cm^2 and thickness 0.3 mm were cut out and placed into Paddington chambers, which are the commonly used set-up for measurements of fluid handling capacity and permeability according to the European Standard EN 13726-1 2002. Each

chamber was closed with a lid when the experiments started. The test chambers with fixed samples and lids were weighed (W_1). Subsequently, 20 mL of saline test solution (8.298 g NaCl and 0.368 g $CaCl_2 \cdot (H_2O)_2$ in 1 L of deionized water) was transferred to each chamber and the weights recorded (W_2). The assembled test chambers were closed and placed on a plastic tray inside a climatic test cabinet at 37 ± 1 °C and 15% RH. The water was in direct contact with the adhesives. After 24 h, the test chambers were removed from the climatic cabinet and left at room temperature for 30 min. After this time, the test chambers were weighed again (W_3). Five repetitions of the test were done for each compositions. Permeability, or WVTR, over 24 h was reported as:

$$WVTR * \Delta t = (W_2 - W_3)/A \quad (1)$$

To determine the water absorption capability of the adhesives, specimens of area (A) 10 cm^2 and thickness 0.3 mm were weighed (W_0) and subsequently immersed in saline test solution for 24 h. After 24h, samples were thoroughly dried with absorbing paper to remove any residual water droplets from the surface and weighed again (W_{24}). Three repetitions of the test were run for each composition. The water absorption over 24 h was reported as:

$$WA * \Delta t = (W_{24} - W_0)/A \quad (2)$$

2.2.4 Linear viscoelastic measurements

Linear viscoelastic (LVE) properties of glycerol-silicone adhesives were measured with a Discovery HR-2 Hybrid Rheometer (TA Instruments) using a parallel-plate geometry 20 mm in diameter. The instrument was set to a controlled strain mode ensured to be within the linear regime. Strain was set at 1%, and frequency sweeps were performed from 100 Hz to 0.01 Hz at 32 °C. Samples thicknesses were 0.6 mm. Measurements were done in triplicate for each composition.

2.2.5 Peel tests on stainless steel plates and pig skin

Samples with a thickness of 0.3 mm were cut in 25 mm x 100 mm rectangles. A TESA 4651 auxiliary tape was then cut in 25 mm wide strips, which in turn were glued to the adhesives. Each adhesive was carefully applied manually to a steel plate and/or pig skin. An automatic roll-down laminating machine (applied pressure 2 kg and rolling speed 300 mm/min) designed for the purpose was used to minimize air inclusion between sample and substrate. Steel plates and/or pig skin with mounted adhesives were then equilibrated for 30 min in a test cabinet at 32 ± 1 °C. Subsequently, peel tests were performed using a Texture Analyser (TA) XT Plus (Micro Systems Ltd., UK). Peel rate and peel angle were set at 5 mm/s and

180°, respectively, for the adhesives mounted on steel plates. For the tests performed on pig skin, peel rate was 5, 1 and 0.1 mm/s, respectively. The peel angle was kept constant at 180°. Five measurements for each composition were performed and results were averaged.

2.2.6 Perspiration simulator and perspiration experiments

The simulator consisted of an artificial skin membrane, mimicking human skin in terms of topography, water contact angle, and sweat pore distribution, was glued to a sweat reservoir. A sweat pore density of 100 cm^{-2} was chosen to represent skin in the abdominal area [33]. Dimensions of artificial skin were 25 mm x 40 mm. Adhesives for the experiments were cut to the same dimensions and then applied to the artificial skin with a defined pressure and over a set time. The reservoir was connected to a custom-made device for controlling the desired height of the water column and thus the desired pressure during the test. The tank was filled with a saline solution of 0.154 M NaCl. The height of the tank was set to achieve a pressure of around 2 kPa, which corresponds to typical pressures observed during perspiration [34]. The tank was connected to the inlet of the reservoir through a tube and the sweat flow was controlled through a valve connected to a flow sensor (Elveflow, France). After 30 min, the sweat flow was stopped and adhesives were peeled off the artificial skin to determine the effect of perspiration on peel force. Peel tests were performed using an Instron 5943. Peel angle and peel rate were set at 90° and 5 mm/s. Three perspiration experiments followed by peel tests were run for each composition. As references, samples were contacted with the artificial skin for 30 min, with no exposure to saline composition, and subsequently peeled off.

2.2.7 Tack tests

A modified version of the Loop Tack method (AST D6195-03) was used for testing. The loop was made of a rectangular strip of printing-paper, dimensions were 25 mm x 175 mm and it was closed with a 25 mm x 25 mm square of double-sided tape. The loop was then mounted in a clamp-fixture on an Instron 5543 and placed with a 2-4 mm gap between the loop and the adhesive. Adhesives were cut to dimensions of 25 mm x 100 mm and mounted on top of a T-shaped platform fixed in the lower grip of the Instron 5543. The loop was lowered until it completely covered the adhesive at a rate of at 5 mm/s, followed by immediate reversal at the same rate, until complete detachment from the sample and return to the initial position. The maximum peak and tack forces were measured from the obtained force curve. Five measurements for each sample were performed and results were averaged.

3. Results and discussion

3.1 Morphology of glycerol-silicone adhesives and determination of glycerol surface area per volume of adhesive

Glycerol-silicone adhesives were produced by applying high shear forces to the glycerol and adhesive premixes. Silicone constitutes the continuous phase with dispersed, discrete droplets of glycerol homogeneously distributed within. Confocal microscopy images of cross-sections of cured adhesives with varying content of glycerol are shown in Fig. 1. Confocal image analysis of the resulting morphology shows that with increased loading of glycerol, the glycerol droplets become larger and more densely distributed despite identical mixing and curing conditions. This is in contrast to results for the previous studies of mixing glycerol into silicone elastomers, where the diameter of the droplet remained constant for a wide range of glycerol loadings undergoing the same mixing and curing procedures [26]. However, the previously investigated elastomers also possess a significant fraction of silica fillers that are believed to stabilize the initial emulsions and thereby also the resulting material. In the current study, the silicone adhesive formulations are filler-free, therefore the stabilizing effect is missing. Furthermore, when glycerol loading increases, more droplets are generated during the emulsion preparation and, additionally, the space between droplets decreases. Therefore, the possibility of droplets agglomeration increases, explaining the larger droplets observed for high-glycerol loading adhesives. The average droplet diameters as function of glycerol loading are shown in SI. To facilitate the understanding of the counterintuitive rheological behavior in the following sections, the surface area of the droplets per total volume of adhesive is required. Knowing the diameter of a glycerol sphere (D_i) and the glycerol volume fraction in a silicone adhesive (φ), the internal surface area ($\sum_i^N A_i$) per volume of adhesive volume (V_{tot}) is calculated by means of simple geometry as:

$$\frac{\sum_i^N A_i}{V_{tot}} = \frac{\varphi \sum_i^N A_i}{\sum_i^N V_i} = \frac{6\varphi \sum_i^N D_i^2}{\sum_i^N D_i^3} \tag{3}$$

since the volume of glycerol can be written as $\sum_i^N V_i = \varphi V_{tot}$ and the diameter of glycerol spheres can be written as $D_i = \sqrt[3]{\frac{6\,V_i}{\pi}}$.

The estimated internal glycerol-silicone surface area per volume of adhesive was determined from averaging over 1,000 droplets. The achieved results are shown in Fig. 2. The internal surface area steadily

increases until it reaches a maximum at 40 phr loading. Subsequently, the extra loading of glycerol no longer increases the internal surface area but rather results in significantly larger droplets - and thereby a reduction of the internal surface area despite the introduction of more glycerol.

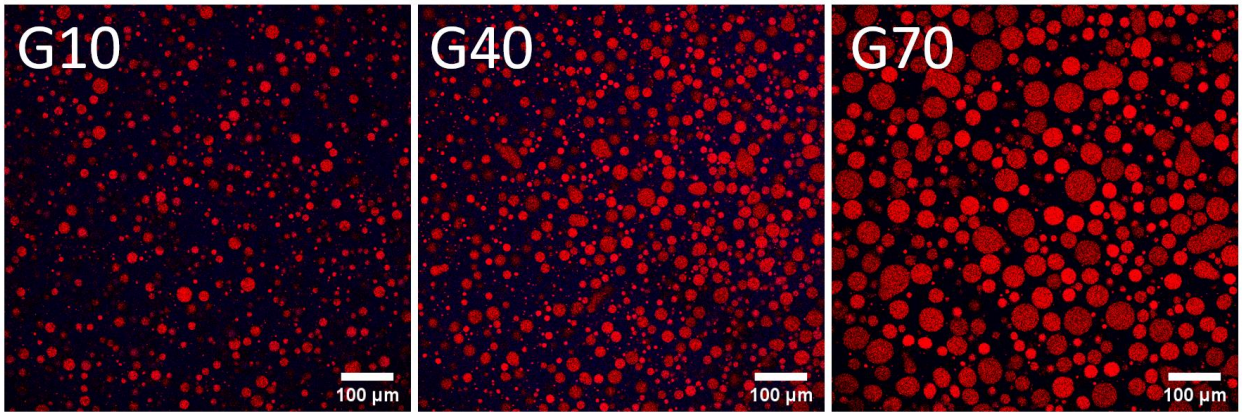

Fig.1. Confocal microscopy images of cured glycerol-silicone adhesives. Higher glycerol amount results in thinner spacing between droplets and in larger droplet diameters. 10, 40 and 70 phr correspond to volume fraction of 7%, 23% and 35%, respectively.

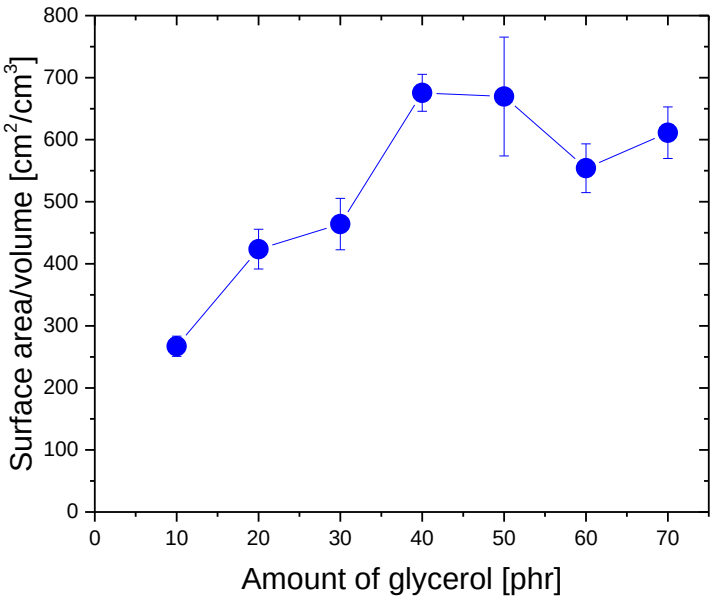

Fig.2. Glycerol surface area per volume of adhesive determined from image analysis of confocal microscopy images.

3.2 Water absorption and permeability

For the glycerol-silicone adhesives, water absorption is an effect of building up osmotic pressure. As water moves down its osmotic potential gradient, it starts to fill the glycerol domains embedded in the silicone

adhesive. It was previously shown that water absorption is more efficient both with respect to rate and total capacity at increasing glycerol loadings for glycerol-silicone elastomers, i.e. more densely cross-linked silicones than the adhesives [26]. It is also known that the softer the silicone, i.e. reduced cross-linking density, the more water can potentially be absorbed by the formulations, as lower elastic stress has to be overcome to expand the glycerol domains [35,36]. Results for water absorption and permeability over 24 h are presented in Fig. 3 and a sketch of the water absorption mechanism is illustrated in Fig. 4. The buildup of sweat at the skin-adhesive interface is unfavorable with respect to adhesion as well as it causes maceration. The glycerol-silicone elastomers allow for removal of the liquid at the interface due to the hygroscopic nature of glycerol. As expected, water absorption increased with increasing glycerol content. Specifically, water uptake increased up to 0.75 g/10 cm^2/day for adhesives containing 50 phr of glycerol compared to the pristine silicone adhesive sample. However, it is surprising that the absorption of adhesives with 60 and 70 phr of glycerol did not increase further, but stabilized at similar level as the 50 phr adhesive. The reduced absorption level after 24 h observed for these samples can be explained by the determined glycerol surface areas per volume of adhesive, reported in Fig. 2. As result of larger average droplet sizes in the higher-glycerol-loading formulations, the glycerol surface area per volume of adhesive did not increase further after 50 phr, but actually decreased for 60 and 70 phr adhesive samples. Hence, the available surface area of glycerol exposed to water during the water absorption experiments is smaller than the available surface area in 40 and 50 phr samples, thus explaining the lower absorption levels after 24 h. In other words, the interfacial area governs the rate of water uptake. Furthermore, since the 60 and 70 phr adhesives did not reach their final absorption capacity after 24 h, the recorded data is transient and this explains the deviation from the behavior of the silicone elastomers, where water uptake scales with loading of glycerol.

The permeability of glycerol-silicone adhesives increased in line with glycerol content as expected. Specifically, an increase of 230% for the 70 phr adhesive samples was observed compared to the pristine silicone sample. When glycerol is introduced in the adhesive formulation, the true thickness of the silicone layer is reduced. As the permeability is highly dependent on the thickness of the silicone layer, the higher the glycerol loading, the thinner the actual silicone barrier that water vapour has to overcome.

In general, the overall enhancement of fluid handling capabilities of glycerol-silicone adhesives in a 24 hours period, facilitated by incorporating emulsified glycerol, was proved, with up to 50 times in water absorption and 3 times increase in permeability compared to the pristine silicone adhesive.

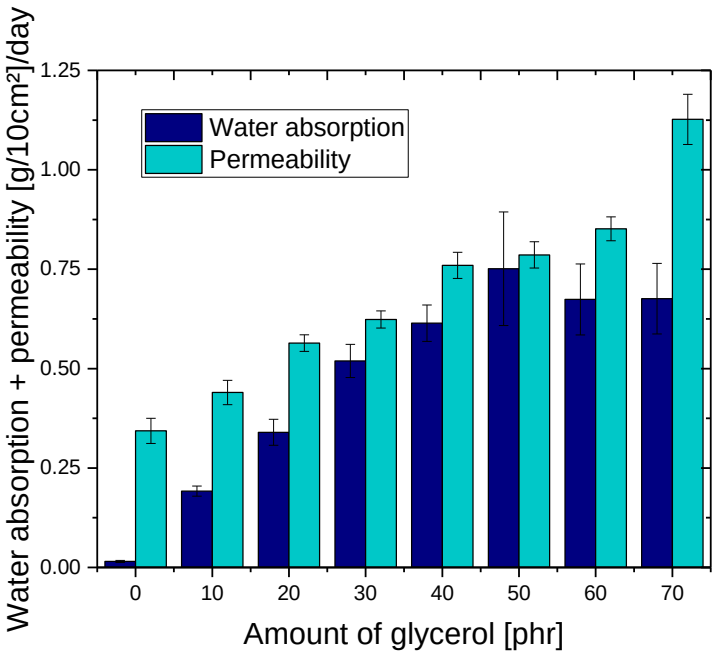

Fig.3. Water absorption and permeability of glycerol-silicone adhesives with different glycerol loadings measured at 37 °C and 15% RH over 24 h. A period of 24 hours is chosen as a representative time for a wound care adhesive. None of the glycerol-silicone adhesives has received their full absorption capacities in the given period due to the transient nature of the adhesives where they simultaneously transport water vapor through the material and water absorption in the glycerol.

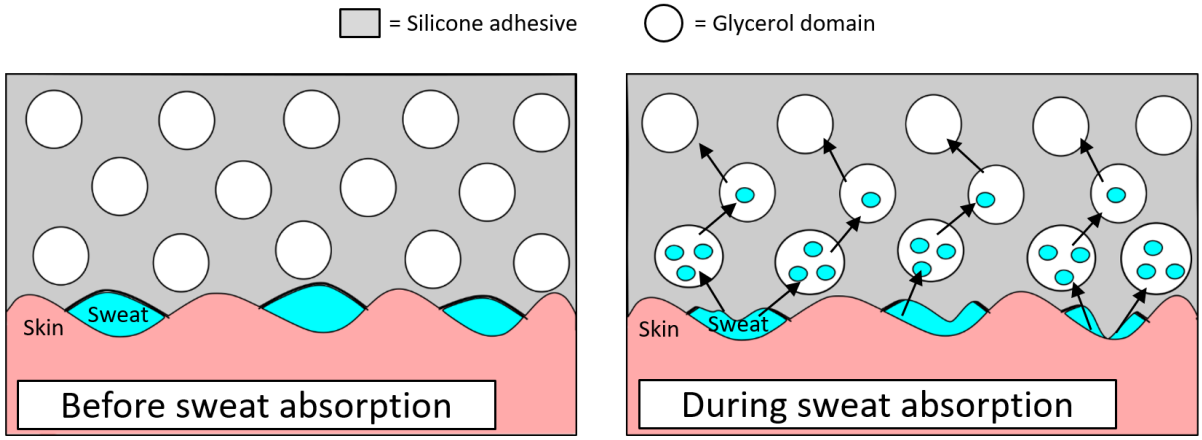

Fig.4. Schematic illustration of the water absorption mechanism by glycerol droplets.

3.3 Linear viscoelastic properties of glycerol-silicone adhesives

Fig. 5A and 5B illustrate storage moduli (G') and dissipation factors (tan δ = G''/G') as a function of frequency for adhesives with glycerol loadings from 0 to 70 phr. Data shows that the adhesives soften in

their linear viscoelastic response (i.e. lower G') to increasing glycerol content, as expected, due to the larger volume fraction of liquid. However, counterintuitively, tan δ decreases across the entire frequency range in line with increased loading of glycerol, thereby indicating that the elastic response compared to the viscous response increases as the samples contain more and more liquid. This can be explained by the elasticity of the cross-linked emulsions having two elastic components, namely the elasticity arising from silicone network and the internal interfacial energies, whereas glycerol does not contribute much to the viscous loss at the given temperature. The results thereby indicate that the interfacial energies constitute a major contribution to elasticity for the soft silicone adhesives.

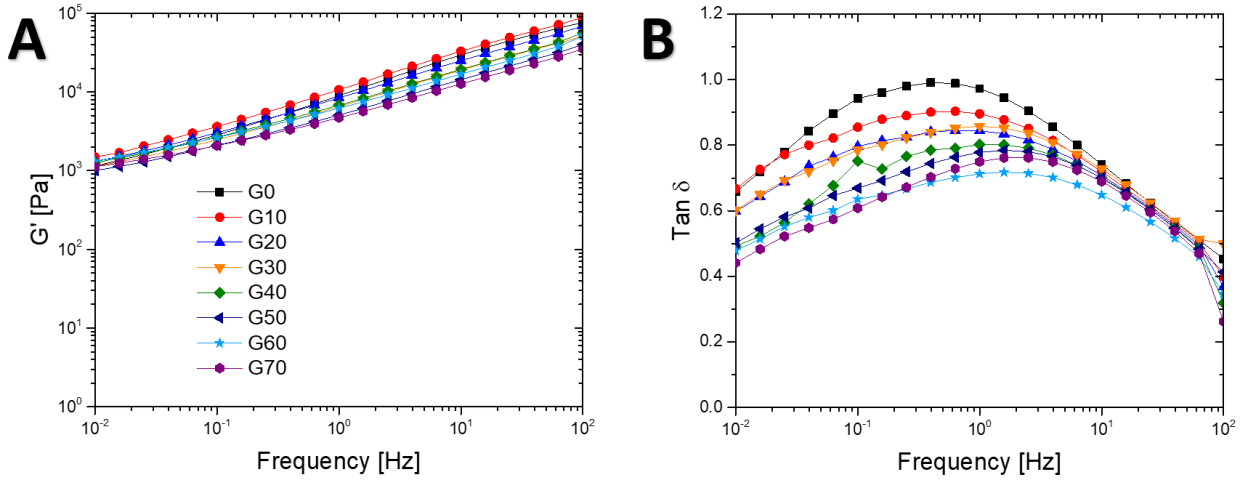

Fig.5. Linear viscoelastic properties of glycerol-silicone adhesives for varying glycerol loadings. Measurements were conducted with controlled strain at 1% and frequency sweeps from 100 Hz to 0.01 Hz at T = 32 °C.

Furthermore, from figure 5B it can be seen that with increased glycerol loading the characteristic relaxation time (as identified by $\tau = \frac{1}{\omega}$ for the frequency for which $\frac{d(\tan\delta)}{d\omega} = 0$, where τ and ω are relaxation time and angular frequency, respectively) decreases. This indicates that - despite the less lossy nature of the adhesive with increased glycerol - the dynamics within the adhesive is speeded up at least a decade from 0 phr to 70 phr. This agrees well with higher mobility at the interfaces compared to the bulk properties.

3.4 Peel force analysis of glycerol-silicone hybrid adhesives on stainless steel plates

Peel forces of adhesives from stainless steel plates and their failure modes were investigated. The results are summarized in Fig. 6A. Initially, a sharp decrease in peel force for the G0 to G20 samples is observed, and then no significant variations in peel forces are detected for increased glycerol loadings up to 50 phr. To explain this behavior, first of all, the true thickness of adhesive layer in contact with the substrate must be considered. The thickness of the adhesive *d* can be related to the peel force F_{peel} via the following equation [10]:

$$\frac{F_{peel}}{dWG_0} = g\left(tan\ \delta_{\omega peel}\right) \quad (4)$$

where *W* is the width of adhesive, G_0 is the zero-shear modulus and ω_{peel} is the frequency of the peeling experiment determined as:

$$\omega_{peel} = V_{peel}/d \quad (5)$$

where V_{peel} is the peel rate of the peeling experiments. *g* is a function, most commonly in the form of *g(x)=x*, and with this assumption the peel force per width of adhesive can be written:

$$\frac{F_{peel}}{W} = dG_0 tan\ \delta_{\omega peel} \quad (6)$$

The true thickness of the adhesive layer instantaneously reduces when glycerol is introduced into the adhesive. This is due to the presence of discrete glycerol droplets, since the thickness of the contacting adhesive is no longer the thickness of the film but rather a distance closely related to the average thickness between droplets. This can explain the rapid drop in peel force from 0 to 10 phr. At the same time, at the peel frequency of (5 mm s^{-1} / 0.30 mm = 17 s^{-1}) there is not much change in *tan δ* or G_0 between 0 and 10 phr. Upon further increases in glycerol loading, the peel force remains constant within experimental uncertainty, due to a combination of no significant reduction in *d* and a small increase in G_0, caused by a stiffening effect from the increased number of droplets in the adhesive. Style *et al* [37,38] showed that surface tension acts to keep liquid inclusions spherical, thus opposing any applied stretch that would make liquid droplets elliptical.

All the compositions, from G0 to G50, exhibited adhesive failure at all frequencies. When glycerol loadings exceeded 50 phr, some instances of cohesive failure were observed, therefore the results were not included in the comparison. Cohesive failures at high loadings are addressed to the large fraction of liquid and thereby less adhesive to withhold the stresses and increased sensitivity to imperfections. As a result, the local stresses on some polymer strands become very high, and cause the adhesive to fail.

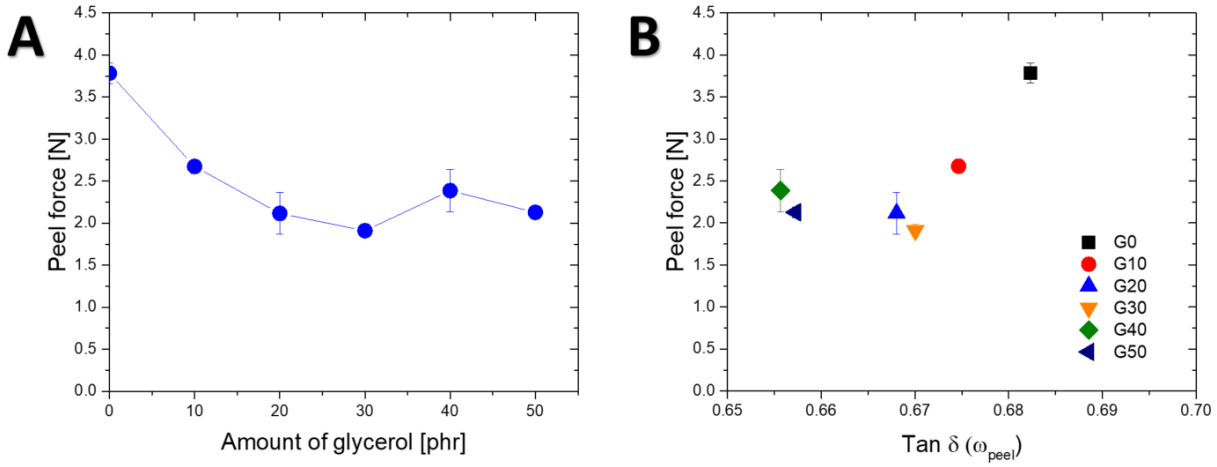

Fig. 6. A) Peel average forces of silicone adhesives with various glycerol loadings on stainless steel plates. Peel force decreased in samples containing glycerol. No significant variations in peel forces were observed from G20 to G50. All compositions from G0 to G50 exhibited adhesive failure mode. B) Peel force vs. loss tangent measured at the peel frequency. Peel force decreases with tan δ from G0 to G20 samples, but remains constant within experimental uncertainty from G20 to G50 samples.

From Fig. 6B it can also be seen that at low loadings the expected scaling of the peel force with *tan δ* prevails whereas for high loadings the scaling departs, probably due to the larger droplets and the resulting interplay between liquid stiffening and larger thickness of contact layer.

3.5 Peel force analysis of glycerol-silicone adhesives on pig skin

Peel forces of glycerol-silicone adhesives from pig skin were investigated at three different peel rates. The results are presented in Fig. 7 and show that the peel force decreases in line with the decreasing peel rate, indicating a correlation between mechanical response and peel velocity. This is in line with prior studies on PSAs [39–43], that have shown that the relationship between peel force (*F*) and peel velocity (*v*) at the same peel angle can be described by:

$$F/b = kv^{n} \quad (7)$$

Where *b* is the width of the adhesive, *k* is a constant that depends on the peel angle and the thickness of the PSA. *n* is a constant related to the intrinsic properties of the PSA [39]. From Fig. 7 it is clear that –

within experimental uncertainty – the peel forces of all the investigated adhesives, including the pristine silicone adhesive, behave identically with variation in peel rate. Therefore, it can be concluded that the intrinsic properties of silicone adhesives are maintained.

In addition, results show that overall there are no remarkable differences in peel forces from the G0 to G50 samples. This behavior is slightly in contrast to the peel forces from steel (Fig. 6), where a drop was observed from 0 to 10 phr reasoned to be due to introducing glycerol in the formulation, which reduces the true thickness of the adhesive layer in contact with the substrate. This deviation can be attributed to the competition between multiple factors. First, as discussed in the previous section, solid stiffening, as a result of glycerol inclusion, increases the experienced modulus. Secondly, as skin has an uneven surface compared to steel, the silicone chains can create a larger, intimate contact area with this substrate due to the high mobility of silicone chains at the interface.

All G0 to G50 compositions exhibited adhesive failure, and we observed instances of cohesion failure for adhesives containing 60 and 70 phr of glycerol. Therefore, these data were omitted.

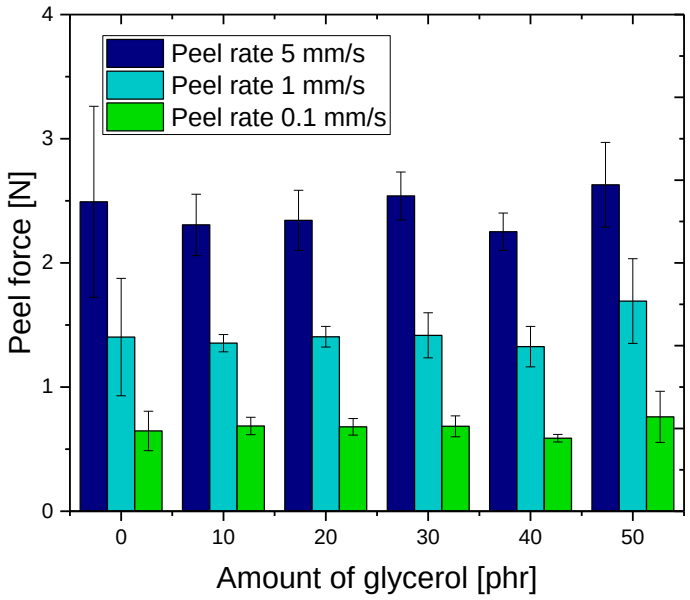

Fig. 7. Peel average forces of silicone adhesives with various glycerol amounts and at various peel rates from pig skin. The adhesive was pulled in the peel direction with an angle of 180° and with a speed of 5, 1 and 0.1 mm/s, respectively, at T = 32°C.

3.6 Perspiration experiments and adhesives' performance characterization

The adhesives' performance under high-perspiration conditions was evaluated using the perspiration simulator ideated by Eiler *et al* [44,45]. This simulator recreates perspirations conditions similar to those occurring on human skin. Sweat glands typically exert pressure of approximately 2 kPa to generate perspiration rates up to 2 µL/cm^2/min [33]. A simplified illustration of the simulator is shown in Fig. 8A. From Fig. 8B it can be seen that variations in peel forces between dry and wet samples were not remarkable. None of the compositions fell off the artificial skin during the experiments, with the single exception of G70. This suggests that almost all adhesives resist ≃ 2 kPa water pressure consistently. Moreover, glycerol-containing adhesives seem less affected (change from dry to sweat) by the simulated sweat pressure than G0. As discussed previously, as a consequence of fluid build-up in the interface skin-adhesive, adhesion failure may occur if the amount of liquid exceeds the absorbing capacity of an adhesive. Glycerol-silicone adhesives showed remarkable resistance during the sweat tests almost momentarily, indicating that glycerol may help remove eventual liquid-build-up at the adhesive-substrate interface, thus maintaining the adhesion level of dry adhesives as result of enhanced permeability.

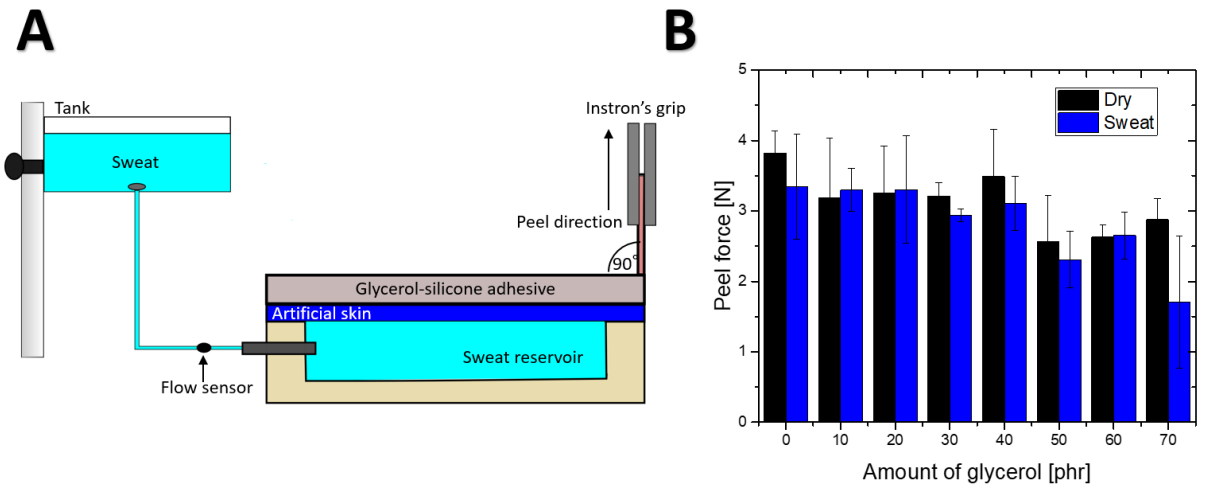

Fig. 8. A) Schematic illustration of the perspiration' experiments' set-up. The height of the tank containing simulated sweat was set to obtain a pressure of ≃ 2 kPa, resulting in a sweat rate of ≃ 2 µL/cm^2/min. Sweat time was set at 30 min. The adhesive was in contact with the artificial skin, which was glued to the sweat reservoir. B) Peel average forces of silicone adhesives with various glycerol amounts on artificial skin. Adhesives were pulled at an angle of 90° and a speed of 5 mm/s. Data revealed no loss of adhesive properties in wet samples compared to dry samples.

3.7 Tack force analysis of glycerol-silicone hybrid adhesives

The tackiness of glycerol-silicone hybrid adhesives was investigated. An illustration of the tack test set-up is shown in Fig. 9A, and the results are shown in Fig. 9B. No significant variations in tack forces were observed when increasing glycerol content in the silicone adhesives. Similarly to the peel force, we believe that the tack force is also affected by the solid stiffening effect. Furthermore, the paper used for the test consisted of high porosity between paper fibers such that the more mobile silicone chains can establish an immediate, large intimate contact area with the paper, as hypothesized in the case of the pig skin (*vide supra*). When glycerol loadings exceeded 50 phr, some instances of adhesive failure were observed, therefore data were omitted.

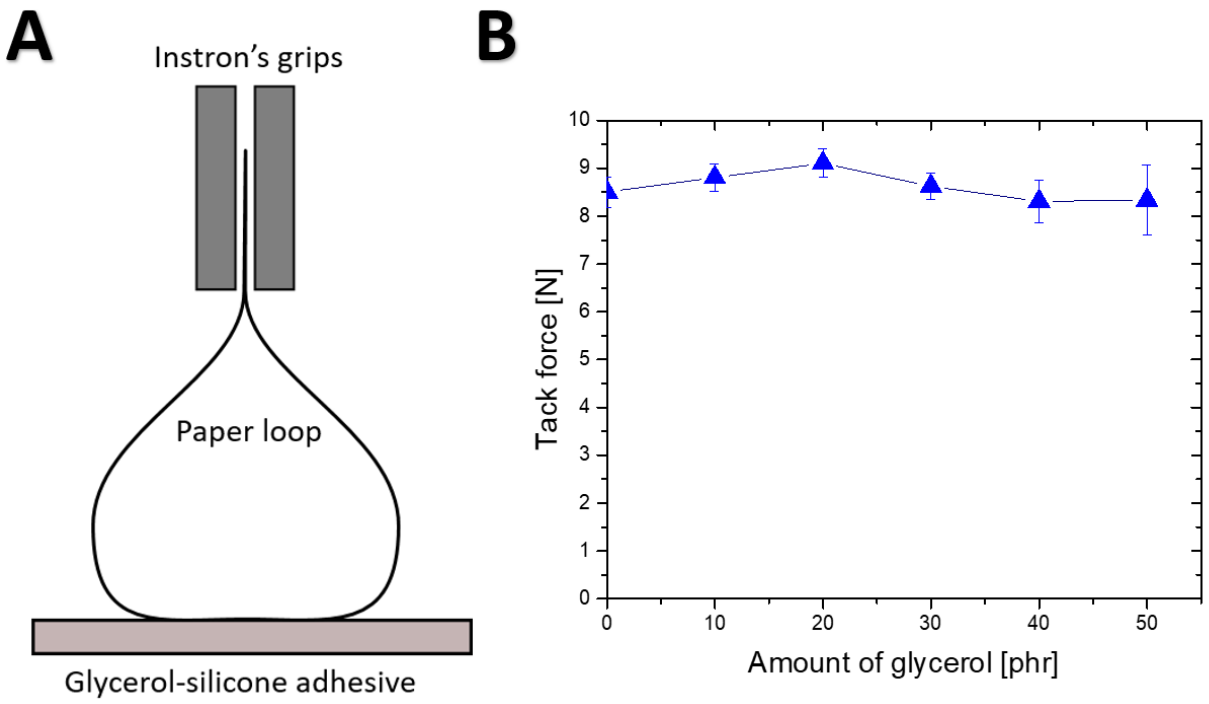

Fig. 9. A) Sketch of the modified Loop Tack method (AST D6195-03). B) Tack average forces of silicone adhesives with various glycerol amounts. No significant variation in tack forces were observed from G0 to G50.

4. Conclusions

A novel glycerol-silicone adhesive was successfully prepared from speed-mixing mixtures of silicone adhesives and glycerol into stable emulsions. Upon cross-linking of the continuous silicone phase in the

emulsions, glycerol-silicone adhesives were obtained, with glycerol embedded in the polymer in the form of discrete droplets. The fluid handling properties of glycerol-silicone adhesives were significantly increased by incorporating glycerol, and peel adhesion tests on stainless steel plates and pig skin revealed that the adhesives' performance was not compromised by incorporating glycerol up to 50 phr. Above 50 phr of glycerol (corresponding to volume fractions of 28%) some instances of cohesive failure were observed. Additionally, perspiration simulation experiments revealed that glycerol-silicone adhesives showed remarkable resistance under harsh conditions. This indicates that glycerol helps removing eventual liquid build-up at the adhesive-substrate interface as a result of enhanced permeability (up to 3 times increased compared to pristine adhesives) and water absorption (up to 50 times compared to pristine adhesives). Lastly, the tackiness was not compromised by adding glycerol to adhesives at a loading up to 50 phr.

The very favorable properties of the prepared adhesives as well as the simplicity of the preparation scheme indicate a simple adhesive with properties partly governed by the used silicone adhesive system as well as the loading of glycerol into it.

5. References

[1] Han G, Ceilley R. Chronic wound healing: a review of current management and treatments. Adv Ther 2017;34:599–610. https://doi.org/10.1007/s12325-017-0478-y.

[2] Carin F, Gonsalves M. Venous leg ulcers. Tech Vasc Interv Radiol 2003;6:132–6. https://doi.org/10.1053/S1089-2516(03)00055-6.

[3] Brem H, Stojadinovic O, Diegelmann RF, Al E. Molecular markers in patients with chronic wounds to guide surgical debridment. Mol Med 2007;13:30–9. https://doi.org/10.2119/2006-00054.Brem.

[4] Cutting KF, White RJ. Maceration of the skin and wound bed. 1: Its nature and causes. J Wound Care 2002;11:275–8. https://doi.org/10.12968/jowc.2002.11.7.26414.

[5] White RJ, Cutting KF. Intervention to avoid maceration of the skin and wound bed. Br J Nurs 2003;12:1186–201. https://doi.org/10.12968/bjon.2003.12.20.11841.

[6] Creton C. Pressure-sensitive adhesives: an introductory course. MRS Bull 2003;28:434–9. https://doi.org/https://doi.org/10.1557/mrs2003.124.

[7] Lin SB, Durfee LD, Ekeland RA, McVie J, Schalau GK. Recent advances in silicone pressure-sensitive adhesives. J Adhes Sci Technol 2007;21:605–23. https://doi.org/10.1163/156856107781192274.

[8] Pizzi A, Mittal KLK. Handbook of Adhesive Technology. 3rd ed. Boca Raton: Taylor & Francis Group; 2017. https://doi.org/10.1201/9781315120942.

[9] Frankaer SMG, Jensen MK, Bejenariu AG, Skov AL. Investigation of the properties of fully reacted unstoichiometric polydimethylsiloxane networks and their extracted network fractions. Rheol Acta 2012;51:559–67. https://doi.org/10.1007/s00397-012-0624-z.

[10] Jensen MK, Bach A, Hassager O, Skov AL. Linear rheology of cross-linked polypropylene oxide as a pressure sensitive adhesive. Int J Adhes Adhes 2009;29:687–93. https://doi.org/10.1016/j.ijadhadh.2008.10.005.

[11] Morris C, Emsley P, Marland E, Meuleneire F, White R. Use of wound dressing with soft silicone adhesive technology. Paediatr Nurs 2009;21:38–43. https://doi.org/10.7748/paed.21.3.38.s32.

[12] Cutting KF. Impact of adhesive surgical tape and wound dressings on the skin, with reference to skin stripping. J Wound Care 2008;17:160–2. https://doi.org/10.12968/jowc.2008.17.4.28836.

[13] Omeara S, Martyn-St James M. Foam dressings for venous leg ulcers. Cochrane Database Syst Rev 2013:CD009907. https://doi.org/10.1002/14651858.CD009907.pub2.

[14] Liu L, Kuffel K, Scott DK, Constantinescu G, Chung HJ, Rieger J. Silicone-based adhesives for long-term skin application: Cleaning protocols and their effect on peel strength. Biomed Phys Eng Express 2018;4:15004. https://doi.org/10.1088/2057-1976/aa91fb.

[15] Dykes PJ, Heggie R, Hill SA. Effect of adhesive dressings on the stratum corneum of the skin. J Wound Care 2001;10:7–10. https://doi.org/10.12968/jowc.2001.10.2.26054.

[16] Satas D. Handbook of pressure sensitive adhesive technology. Int J Adhes Adhes 1999;20. https://doi.org/10.1016/S0143-7496(99)00067-6.

[17] Minghetti P, Cilurzo F, Casiraghi A. Measuring adhesive performance in transdermal delivery systems. Am J Drug Deliv 2004;2:193–206. https://doi.org/10.2165/00137696-200402030-00004.

[18] Kenney JF, Haddock TH, Sun RL, Parreira HC. Medical-grade acrylic adhesives for skin contact. J Appl Polym Sci 1992;45:355–61. https://doi.org/10.1002/app.1992.070450218.

[19] Renvoise J, Burlot D, Marin G, Derail C. Peeling of PSAs on viscoelastic substrates: A failure criterion. J Adhes 2007;83:403–16. https://doi.org/10.1080/00218460701282554.

[20] Renvoise J, Burlot D, Marin G, Derail C. Adherence performances of pressure sensitive adhesives on a model viscoelastic synthetic film: A tool for the understanding of adhesion on the human skin. Int J Pharm 2009;368:83–8. https://doi.org/10.1016/j.ijpharm.2008.09.056.

[21] Cunningham DD, Lowery MG. Moisture vapor transport channels for the improved attachment of a medical device to the human body. Biomed Microdevices 2004;6:149–54. https://doi.org/10.1023/B:BMMD.0000031752.63215.61.

[22] Frassica MT, Jones SK, Diaz-Rodriguez P, Hahn MS, Grunlan MA. Incorporation of a silicon-based polymer to PEG-DA templated hydrogel scaffolds for bioactivity and osteoinductivity. Acta Biomater 2019;99:100–9. https://doi.org/10.1016/j.actbio.2019.09.018.

[23] Fay F, Hawkins ML, Rehel K, Grunlan MA, Linossier I. Non-toxic, anti-fouling silicones with variable PEO-silane amphiphile content. Green Mater 2016;4:53–62. https://doi.org/10.1680/jgrma.16.00003.

[24] Zouaghi S, Barry ME, Bellayer S, Lyskawa J, André C, Delaplace G, et al. Antifouling amphiphilic silicone coatings for dairy fouling mitigation on stainless steel. Biofouling 2018;34:769–83. https://doi.org/10.1080/08927014.2018.1502275.

[25] Rajendra V, Chen Y, Brook MA. Structured hydrophilic domains on silicone elastomers. Polym Chem 2010;1:312–20. https://doi.org/10.1039/b9py00220k.

[26] Mazurek P, Hvilsted S, Skov AL. Green silicone elastomer obtained from a counterintuitively stable mixture of glycerol and PDMS. Polymer 2016;87:1–7. https://doi.org/10.1016/j.polymer.2016.01.070.

[27] Mazurek P, Ekbrant BEF, Madsen FB, Yu L, Skov AL. Glycerol-silicone foams – Tunable 3-phase elastomeric porous materials. Eur Polym J 2019;113:107–14. https://doi.org/10.1016/j.eurpolymj.2019.01.051.

[28] Woolfson AD, Malcolm RK, Gallagher RJ. Design of a silicone reservoir intravaginal ring for the delivery of oxybutynin. J Control Release 2003;91:465–76. https://doi.org/10.1016/S0168-3659(03)00277-3.

[29] Malcolm RK, McCullagh SD, Woolfson AD, Gorman SP, Jones DS, Cuddy J. Controlled release of a model antibacterial drug from a novel self-lubricating silicone biomaterial. J Control Release 2004;97:313–20. https://doi.org/10.1016/j.jconrel.2004.03.029.

[30] Murphy PS, Evans GRD. Advances in wound healing: a review of current wound healing products. Plast Surg Int 2012:190436. https://doi.org/10.1155/2012/190436.

[31] Mazurek P, Brook MA, Skov AL. Glycerol-silicone elastomers as active matrices with controllable release profiles. Langmuir 2018;34:11559–66. https://doi.org/10.1021/acs.langmuir.8b02039.

[32] Mazurek P, Yu L, Gerhard R, Wirges W, Skov AL. Glycerol as high-permittivity liquid filler in dielectric silicone elastomers. J Appl Polym Sci 2016;133:1–8. https://doi.org/10.1002/app.44153.

[33] Sonner Z, Wilder E, Heikenfeld J, Kasting G, Beyette F, Swaile D, et al. The microfluidics of the eccrine sweat gland, including biomarker partitioning, transport, and biosensing implications. Biomicrofluidics 2015;9:031301. https://doi.org/10.1063/1.4921039.

[34] Choi J, Xue Y, Xia W, Ray TR, Reeder JT, Bandodkar AJ, et al. Soft, skin-mounted microfluidic systems for measuring secretory fluidic pressures generated at the surface of the skin by eccrine sweat glands. Lab Chip 2017;17:2572–80. https://doi.org/10.1039/c7lc00525c.

[35] Larsen AL, Hansen K, Sommer-Larsen P, Hassager O, Bach A, Ndoni S, et al. Elastic properties of nonstoichiometric reacted PDMS networks. Macromolecules 2003;36:10063–70. https://doi.org/10.1021/ma034355p.

[36] Ndoni S, Kramer O. Longest relaxation time of linear polybutadiene chains trapped in rubber networks. Europhys Lett 1997;39:165–70. https://doi.org/10.1209/epl/i1997-00330-9.

[37] Style RW, Boltyanskiy R, Allen B, Jensen KE, Foote HP, Wettlaufer JS, et al. Stiffening solids with liquid inclusions. Nat Phys 2015;11:82–7. https://doi.org/10.1038/nphys3181.

[38] Eshelby JD. The determination of the elastic field of an ellipsoidal inclusion, and related problems. Proc R Soc Lond A Math Phys Sci 1957;241:376–96. https://doi.org/10.1007/1-4020-

4499-2_18.

[39] Zhou M, Tian Y, Pesika N, Zeng H, Wan J, Meng Y, et al. The extended peel zone model: effect of peeling velocity. J Adhes 2011;87:1045–58. https://doi.org/10.1080/00218464.2011.609455.

[40] Wei J, Hutchinson JW. Interface strength, work of adhesion and plasticity in the peel test. Int J Fract 1998;93:315–33. https://doi.org/https://doi.org/10.1023/A:1007545200315.

[41] Blum FD, Metin B, Vohra R, Sitton OC. Surface segmental mobility and adhesion - Effects of filler and molecular mass. J Adhes 2006;82:903–17. https://doi.org/10.1080/00218460600875920.

[42] Marin G, Derail C. Rheology and adherence of pressure-sensitive adhesives. J Adhes 2006;82:469–85. https://doi.org/10.1080/00218460600713618.

[43] Du J, Lindeman DD, Yarusso DJ. Modeling the peel performance of pressure-sensitive adhesives. J Adhes 2004;80:601–12. https://doi.org/10.1080/00218460490477044.

[44] Eiler J, Hansen D, Bingöl B, Hansen K, Heikenfeld J, Thormann E. In vitro evaluation of skin adhesives during perspiration. Int J Adhes Adhes 2020;99. https://doi.org/10.1016/j.ijadhadh.2020.102574.

[45] Hou L, Hagen J, Wang X, Papautsky I, Naik R, Kelley-Loughnane N, et al. Artificial microfluidic skin for in vitro perspiration simulation and testing. Lab Chip 2013;13:1868–75. https://doi.org/10.1039/c3lc41231h.